Coupling to the Lower-hybrid Resonance

S. Puri and M. Tutter

Max-Planck-Institut für Plasmaphysik, 8046 Garching, FRG

The transmission coefficient of a plane electromagnetic wave into a cold, inhomogeneous, magnetized, deuterium plasma half-space and its eventual absorption at the lower-hybrid layer is computed numerically for a wide range of parameters. It is found that TM (transverse magnetic) waves incident at small angles with the vacuum-plasma interface couple into the plasma provided that $\omega/\omega_{ci} \lesssim 20$. Assuming that coupling to the lower-hybrid resonance in the cold-plasma approximation is an indication of accessibility to the ion-cyclotron-harmonic waves in the hotplasma case, an alternative statement of the results obtained is that efficient coupling is possible from the second till the twentieth harmonic of the ion gyrofrequency using an antenna that launches TM waves at an approximately grazing incidence on the plasma surface. Simple configurations for coupling rf energy into thermonuclear plasma are suggested.

1. Introduction

In the wake of the success in plasma confinement in toroidal machines, the problem of igniting thermonuclear plasmas has assumed added importance. Radio-frequency heating has long been a promising contender for realizing this goal. In the cold-plasma approximation, the two possible methods of ion heating exploit the ion-cyclotron and lower-hybrid resonances, respectively. Of these two possibilities, only the latter is feasible if we wish to avoid magnetic field deformations using a "magnetic beach" configuration. The hot-plasma counterpart of the lower-hybrid resonance is the ion-Bernstein modes which have regions of strong absorption, in the presence of magnetic field gradients, at the harmonics of the ion gyrofrequency. Before the extremely complicated question of ion-cyclotron harmonic heating can be tackled, it would be instructive to attempt a detailed understanding of the lower-hybrid heating.

Central to the problem of rf heating is the mechanism for coupling the energy from an antenna located in the vacuum, into the resonant region in the interior of the plasma where absorption eventually occurs. The electromagnetic wave launched by the antenna, during its advance into the magnetized plasma of gradually increasing density converts into a slow electrostatic wave, eventually encountering a region of very high refractive index and low group velocity in the vicinity of the lower-hybrid resonance. Some dissipation mechanism such as colli-

sions would then result in efficient absorption of the wave energy. The important question arises: what fraction of the energy launched by the antenna is admitted into the plasma?

Though precisely stated, the solution of this problem presents a formidable analytical challenge. A really satisfactory approach remains elusive despite some noteworthy attempts.

For optimum transmission it is clearly desirable that n_r, the refractive index in the direction of the density gradient be real everywhere between the antenna and the resonant layer. From an analysis of the cold-plasma dispersion relation, Stix[1] concluded that this condition for propagation is satisfied (except in a narrow region of inconsequential importance near the plasma edge) if

$$n_z > 2\,(1 + \omega_{pe}^2/\omega_{ce}^2) \tag{1.1}$$

where n_z is the refractive index along the static magnetic field direction. Through certain algebraic improvements, Parker[2] and Golant[3], respectively, arrive at the following less stringent variations of the propagation condition,

$$n_z > 1 + \omega_{pe}/\omega_{ce} \tag{1.2}$$

and

$$n_z > 1 + (\omega_{pe}/\omega_{ce})^2 . \tag{1.3}$$

The methods suggested for obtaining the required longitudinal retardation include the *Stix coil*[1], *gap excitation*[2] or a *slow wave structure*[3, 4]. With this provision one may anticipate using the WKB theory that the wave propagates without reflection provided that the refractive index is a slowly varying function of position. Although perhaps valid in the intermediate region, this so-called adiabaticity con-

dition is severely violated both at the vacuum-plasma interface [2, 3] and near the resonant layer in the interior of the plasma [1]. Using singular turning point analysis, Budden [5] and Stix [1] have shown that the wave propagates from the intermediate region to the hybrid layer and is completely absorbed without reflection.

The crucial question of a possible mismatch at the vacuum-plasma interface is treated in almost identical manners by Parker [2] and Golant [3]. Paradoxically in their analyses, the thin evanescent region near the plasma edge, which was considered inconsequential by Stix [1], assumes critical importance. Unfortunately, they both seem to err in neglecting the E_z' term [6] in comparison with the E_z term in the differential equation for the electric field. This oversight would render their calculations of plasma impedance incorrect.

In recognition of the inadequacy of the WKB theory and in the absence of a satisfactory alternative for an analytical approach, several authors have resorted to purely numerical means for studying the hybrid resonances [5, 7, 8]. Though lacking the elegance of an analytical solution, essentially exact results can be obtained through the use of numerical computations.

In this paper transmission of a plane electromagnetic wave into a cold, inhomogeneous, magnetized, deuterium plasma half-space, as well as its eventual absorption at the lower-hybrid layer, is computed numerically for a wide range of parameters. This work distinguishes itself from previous such attempts both in the scope and the accuracy of the results obtained. The case of oblique incidence is treated employing the complete cold-plasma dispersion and the transmission co-efficient is calculated for a wide range of parameters including the angle of incidence, wave polarization, collision frequency, ratio of electron-plasma to electron-cyclotron frequency, and for several density gradients.

By far the most significant point of departure in our approach to coupling rf energy into thermonuclear plasmas is the awareness of the fact that in an actual reactor, erection of any structure, whatsoever, is undesirable even if not altogether ruled out. In the absence of such structures, the plasma and the reactor walls constitute a partially filled waveguide in which (barring some pathological circumstances) n_z is necessarily less than unity. In Ref. [9] it is shown that in such a plasma-filled waveguide quasi-TEM coaxial waveguide-like modes are invariably present with $n_z \lesssim 1$ even when the free-space wavelength of the rf field greatly exceeds the transverse waveguide dimensions.

Therefore, we shall confine our attention [10] to the case when the electromagnetic wave is incident on the plasma surface at angles between 0 and $\pi/2$. Although this choice is in obvious conflict with the criteria of $(1.1) - (1.3)$, we shall see that it is indeed possible to create conditions of efficient coupling for a broad range of parameters pertinent to the thermonuclear conditions, thereby confirming the validity of the antenna configurations suggested in the preliminary results of Reference [11].

The density profile is taken into account using a stratified plasma model. This model becomes exact as the number of slabs tends to infinity and the thickness of each slab approaches zero. In practice, an acceptable approximation is obtained by making each plasma slab much thinner than the local value of the wavelength. The absorption mechanism considered is the momentum transfer collisions between electrons and ions using the Langevin model.

Beyond the inaccuracies inherent in the Langevin collision model and the stratification of the plasma profile, the problem can be treated exactly. For the four plasma waves occuring in each slab, four boundary conditions exist requiring the continuity of the tangential electric and magnetic fields.

2. The Method of Solution

Figure 1 shows the orientation of the axes used in the computations. The plasma half-space extends from $x = 0$ to $x = \infty$, the static magnetic field B_0
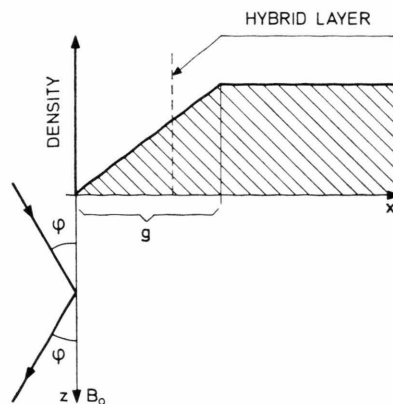

Fig. 1. The co-ordinate system.

is along the z-direction and the angle of incidence φ is defined as the angle between the vacuum wave vector and the plasma surface. All field quantities are assumed to possess space and time dependence $\exp i(k_x x + k_z z - \omega t)$ with no variation in the y-direction. The full cold-plasma dielectric tensor used in a plasma slab of uniform electron density n_e is,

$$K = \begin{pmatrix} K_\perp & -iK_x & 0 \\ iK_x & K_\perp & 0 \\ 0 & 0 & K_\parallel \end{pmatrix} \qquad (2.1)$$

where

$$K_\perp = 1 - \frac{\omega_{pi}^2}{\omega^2 - \omega_{ci}^2} - \frac{\omega_{pe}^2}{\omega^2 - \omega_{ce}^2} \qquad (2.2)$$

$$K_x = \frac{\omega_{ci}}{\omega} \frac{\omega_{pi}^2}{\omega^2 - \omega_{ci}^2} - \frac{\omega_{ce}}{\omega} \frac{\omega_{pe}^2}{\omega^2 - \omega_{ce}^2} \qquad (2.3)$$

$$K_\parallel = 1 - \omega_{pi}^2/\omega^2 - \omega_{pe}^2/\omega^2 . \qquad (2.4)$$

$\omega_{pi}^2 = n_e e^2/M \varepsilon_0$, $\omega_{pe}^2 = n_e e^2/m_\nu \varepsilon_0$, $\omega_{ci} = e B_0/M$ and $\omega_{ce} = e B_0/m_\nu$. In conformity with the use of the Langevin equation, m_ν in the above equations is defined as

$$m_\nu = m(1 + i \nu_{ei}/\omega) \qquad (2.5)$$

where m is the electron mass and ν_{ei} is the electron-ion momentum transfer collision frequency according to Spitzer [12]. We shall specify ν_{ei} by the equivalent temperature T. This results in a variable value of ν_{ei} across the inhomogeneous plasma column. It should, however, be borne in mind that apart from specifying ν_{ei}, T does not imply any departure from the cold-plasma theory. The mean value of ν_{ei} averaged in the region $0 < x < g$ will be denoted by $\langle \nu_{ei} \rangle$.

The plasma density is assumed to rise linearly from $n_e = 0$ to $n_e = n_{max}$ as x increases from $x = 0$ to $x = g$ and thereafter stays constant as shown in Figure 1. The region $0 < x < g$ is stratified into 99 slabs while $x > g$ forms the 100th slab.

Defining $\tilde{K}_\perp = K_\perp - n_z^2$, the dispersion relation may be written as

$$n_x^2 = \frac{K_\perp \tilde{K}_\perp - K_x^2 + K_\parallel \tilde{K}_\perp}{2 K_\perp} \qquad (2.6)$$

$$\pm \left[\left(\frac{\tilde{K}_\perp K_\perp - K_x^2 + K_\parallel \tilde{K}_\perp}{2 K_\perp} \right)^2 + \frac{K_\parallel}{K_\perp} (K_x^2 - \tilde{K}_\perp^2) \right]^{1/2}.$$

Corresponding to the four roots of this equation, the x-components of the electric fields associated with the four waves in a given plasma slab are

$$E_{x\pm}^{f,s} = \hat{E}_\pm^{f,s} \exp i(k_{x\pm}^{f,s} x + k_z z - \omega t) \qquad (2.7)$$

while E_y, E_z, H_x, H_y, H_z may be expressed in terms of E_x using the dielectric tensor and the Maxwell's equations. The indices f (fast) and s (slow) correspond respectively to the smaller and the larger roots of n_x^2. For each of the roots n_x^2, the two waves associated with $\pm n_x$ are labled plus and minus respectively so that $n_{x+} = -n_{x-}$. The slow wave is the quasi-extraordinary mode which encounters the resonance at the lower-hybrid layer as $K_\perp \to 0$. In the slab to the right of $x = g$, there are only two waves, one fast and one slow, each of which decays for increasing x, there being no sources at infinity. In the vacuum region, there is an incident wave (either TM or TE) of unit amplitude and two reflected waves, one TM and one TE.

If R_{TM} and R_{TE} are the amplitudes of the reflected TM and TE waves, the total reflected energy is given by $R^2 = |R_{TM}|^2 + |R_{TE}|^2$, so that the fractional transmitted energy is given by $(1 - R^2)$.

One may readily verify that the number of undetermined quantities exactly equals the boundary conditions. The resultant set af 400 complex, linear, algebraic equations is solved using standard computational methods. In order to obtain maximum computational accuracy, the slab widths Δx are adjusted so that the phase change $\Delta \Phi = |k_x^s \Delta x|$ in each slab is approximately equal. Typically for the case $g = 1$ cm, $\Delta \Phi / 2 \pi < 1/30$ in each of the slabs while in the slabs lying in the immediate vicinity of the hybrid layer $\Delta \Phi / 2 \pi < 1/300$. In the neighbourhood of the resonance $|\mathrm{Im}(k_x^s)| \gg 1$ and quantities like $\exp[i(k_x^s x)]$ create overflow problems. This difficulty is circumvented by transforming the axis $x = 0$ to the hybrid layer during the computational phase.

Checks performed on the continuity of the normal components of the Poynting vector $1/2 (E \times H^*)_x$, electric displacement $\varepsilon_0 (K \cdot E)_x$ and magnetic induction $\mu_0 H_x$ across each of the slab boundaries indicated a computational accuracy exceeding one part in a million. By far the most stringent test involves establishing in each plasma slab the equality of divergence of the Poynting vector $\nabla \cdot [1/2 (E \times H^*)]$ with the rate of change of stored energy $- (i \omega/2) [\varepsilon_0 (E^* \times K \times E)^* - \mu_0 H^2]$ with an accuracy better than one part in a thousand. Convinced that the computations by themselves introduce no considerable error, we are in a position to test the accuracy of the slab model itself. To this effect the

computations for the case $T = 3 \times 10^4 \,^{\circ}$K, $g = 1$ cm, $\omega/\omega_{ci} = 10$ were repeated with 67, 51, 34 and 26 slabs, respectively. The maximum deviation of $\pm 15\%$ occurs in the region where $(1 - R^2) \sim 0.5$ and uniformly tapers off to less than $\pm 3\%$ for $0.1 < (1 - R^2) < 0.9$.

3. A representative Case

In this section a representative case with parameters of Table 1 and $\varphi = 1^{\circ}$ will be studied in

Table 1. Parameters used in the representative calculations of Section 3.

Gas used	Deuterium
Magnetic field, B_0	100 kG
Ion-cyclotron frequency, f_{ci}	76×10^6 Hz
RF frequency, f	760×10^6 Hz
Vacuum wavelength, λ_0	40 cm
Plasma density at the lower-hybrid resonance, n_{lh}	2.7×10^{13} cm^{-3}
Maximum plasma density, $n_{max} = 1.3 \, n_{lh}$	3.5×10^{13} cm^{-3}
Temperature, T	$3 \times 10^4 \,^{\circ}$K
$\langle \nu_{ei} \rangle / \omega$	10^{-2}
Profile width, g	1 cm

detail. The computed transmission co-efficient is 0.98, i. e., almost the entire incident energy goes into the plasma. It will be presently shown that about 81% of this energy couples into the slow wave and is absorbed near the lower-hybrid resonance, while the rest is coupled into the fast wave and propagates practically unattenuated. The propagation constant k_x for this case is shown in Fig. 17 a and is real everywhere except for a narrow region near the plasma edge [13].

The real part of the x-component of the electric field is sketched in Figure 2. The slow wave field increases rapidly reaching an amplitude of over 100 times the vacuum value at the hybrid layer and then drops suddenly. Starting with a almost equal value, the fast wave field stays constant and is impervious to the presence of the hybrid layer.

The x-component of the real part of the Poynting vector $[1/2(E \times H^*)]_x$ has a sharp drop at the hybrid layer where the dissipation density $-\nabla \cdot [1/2(E \times H^*)]$ registers a strong peak (Figure 3) [14]. Assuming that to the right of the hybrid layer, energy is carried by the fast wave only, we can estimate from Fig. 3 that of the total energy

coupled into the plasma about 81% goes into exciting the slow wave and 19% into the fast wave. Although the relative energies coupled into the slow and fast waves varies in a complicated manner as a function of φ and ω_{pe}/ω_{ce}, for TM polarization it was found for the parameter range studied that always more than 59% of the total energy coupled goes into the slow wave. For TE polarization, on the other hand, the maximum energy coupled into the slow wave is only 31%.

The energy density $\varepsilon = (1/4)[\varepsilon_0 E^* \cdot \partial(\omega K)/\partial \omega \cdot E + \mu_0 H^2]$ at the hybrid layer is over ten thousand times larger than the vacuum value (Figure 4). Thus in a waveguide partially filled with plasma, only a small fraction of the total energy resides in the vacuum region, while most of it is concentrated near the hybrid layer. Since the fractional dissipation of energy in the plasma may be much less than the dissipation of the vacuum energy by the metal walls, the quality factor

$$Q = \omega \int_V \varepsilon \, d^3x / \int_V - \nabla \cdot [1/2(E \times H^*)] \, d^3x$$

of a plasma filled waveguide may be greater than the empty waveguide Q [9].

As expected, near the hybrid layer the relative energy $(\varepsilon_i/\varepsilon)$ stored in the ions is much larger than the relative energy $(\varepsilon_e/\varepsilon)$ in the electron component (Figure 5). The ratio $(\varepsilon_i/\varepsilon_e) \sim 37$ and is precisely the value calculated from simple analytical considerations neglecting the longitudinal electric field E_z. If in addition to the electron-ion collisions, some other mechanisms (like cyclotron-harmonic absorption in a hot plasma) for directly dissipating the ion energy were available, both the dissipation density characteristics and the waveguide Q will be profoundly altered. Figure 5 also shows the relative energy $(\varepsilon_v/\varepsilon)$ in the electromagnetic field.

The group velocities $v_{gx}^{f,s} = \partial\omega/\partial k_x^{f,s}$ and $v_{gz}^{f,s} = \partial\omega/\partial k_z^{f,s}$ are shown in Figure 6. For the slow wave both v_{gx} and v_{gz} become progressively smaller as the hybrid layer is approached. However, since the ratio v_{gz}/v_{gx} is always increasing, an energy pulse launched at the plasma edge and travelling with the group velocity of the slow wave advances at a monotonically decreasing angle with the static magnetic field direction as shown in Figure 7 [2, 15, 16].

4. Varying the Parameters

In this section the effect of varying the collision frequency ν_{ei}, the ratio ω_{pe}/ω_{ce} of electron-plasma
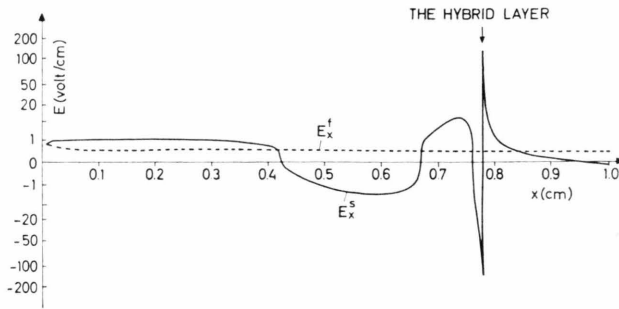
Fig. 2. The real part of the x-component of the electric field vs x for both the slow and the fast waves for the representative case of Section I. (The vertical scale is cubically compressed.)
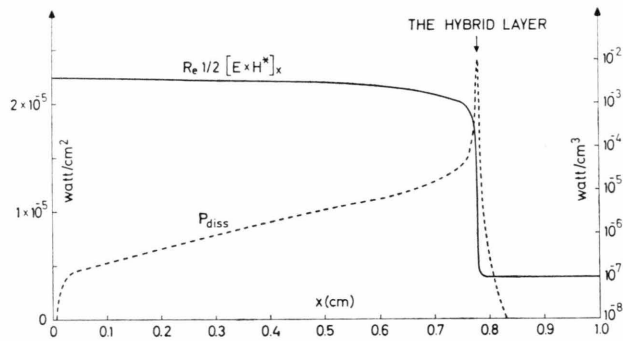

Fig. 5. Relative energy densities $\varepsilon_i/\varepsilon$, $\varepsilon_e/\varepsilon$ and $\varepsilon_V/\varepsilon$ in the ions, the electrons and the electromagnetic field, respectively.

Fig. 3. Real part of the x-component of the Poynting vector $[1/2(E \times H^*)]_x$ and the dissipation density $-\nabla \cdot [1/2(E \times H^*)]$ vs. x.

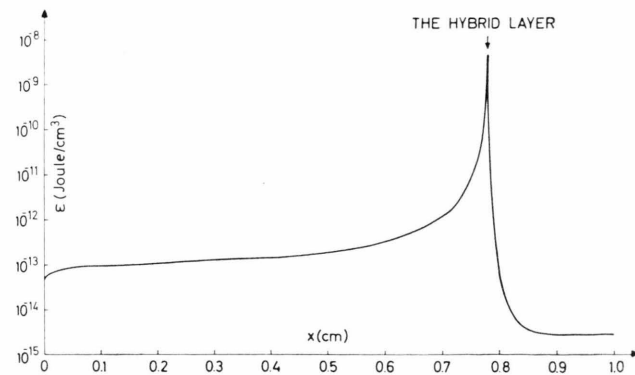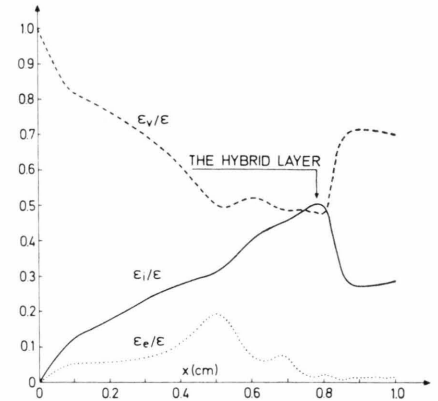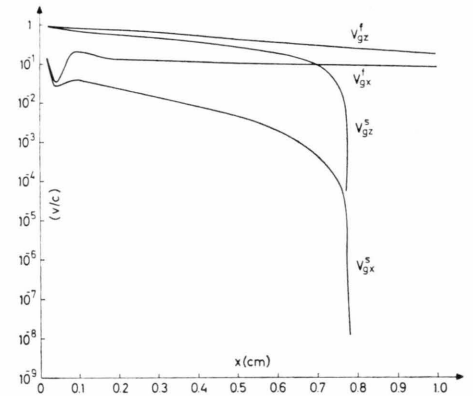Fig. 6. The x and z-components v_{gx}/c and v_{gz}/c of the normalized group velocities for both the fast and the slow waves.

Fig. 4. Energy density $\varepsilon = 1/4[\varepsilon_0 E^* \cdot \partial(\omega K)/\partial\omega \cdot E + \mu_0 H^2]$ vs x.
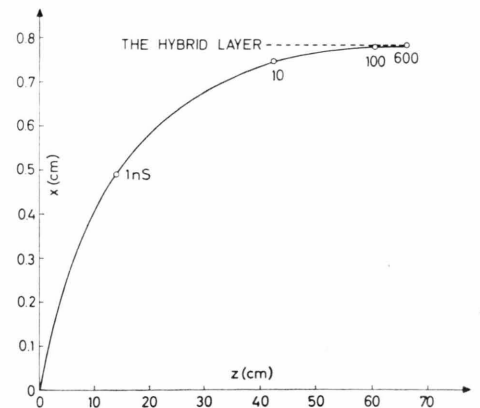

Fig. 7. Propagation of an energy pulse travelling with the group velocity of the slow wave from the plasma edge to the hybrid layer.

to electron-cyclotron frequency, and the profile width "g" will be studied both for the TM and TE polarizations for incidence angle φ varying between $0.01°$ and $89°$. The ratio n_{max}/n_{lh} of the maximum electron density to the density at the hybrid layer, is kept fixed equal to 1.3 through all the computations in this paper.

(a) The Collision Frequency

Figure 8 shows the transmitted energy as a function of φ for several values of T for an incident TM
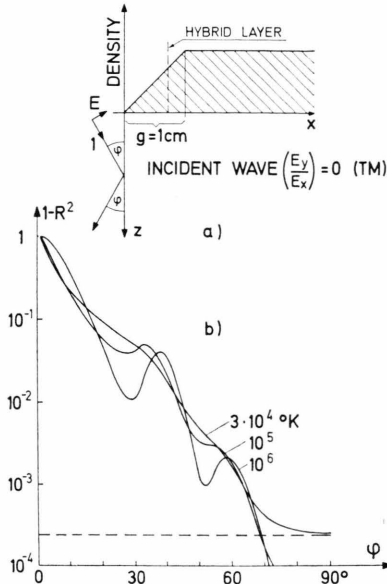

Fig. 8. Transmission coefficient $(1-R^2)$ as a function of φ and T for an incident TM wave using all other parameters as given in Table 1.

wave using the parameters of Table 1. For the sake of comparison, the energy transmission coefficient into stainless steel is also shown (dashed line). It is seen that the effect of decreasing ν_{ei} or increasing T ($T = 10^6$ corresponds to $\langle \nu_{ei} \rangle/\omega \sim 10^{-4}$), is to introduce fluctuations in the transmission co-efficient while the general trend of rapidly decreasing transmission [17] with increasing φ is largely unaffected. Similar curves for an incident TE wave are shown in Figure 9. In this case maximum transmission occurs near $\varphi \sim 30°$ which is certainly in variance with a simple WKB model. The effects caused by changing T are akin to the TM case already decribed.

(b) Varying ω_{pe}/ω_{ce}

In a fusion machine, ion-cyclotron harmonic heating must replace the lower-hybrid heating [18]. Since

the rf frequency in this case is unlikely to exceed the tenth harmonic of the ion-cyclotron frequency, all the preceding calculations as well as the calculations in Ref. [9] were performed with $\omega/\omega_{ci} = 10$, with the corresponding [19] value of $\omega_{pe}/\omega_{ce} = 0.17$. Assuming that for lower values of ω_{pe}/ω_{ce} the accessibility is easier, the choice of $\omega/\omega_{ci} = 10$ presents the most extreme situation likely to be faced in a thermonuclear plasma.
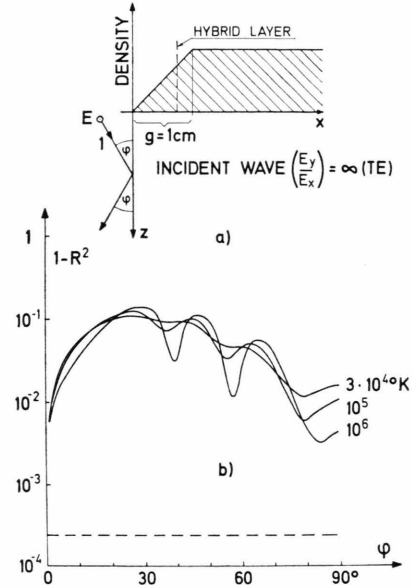

Fig. 9. Transmission coefficient as a function of φ and T for an incident TE wave using all other parameters as given in Table 1.
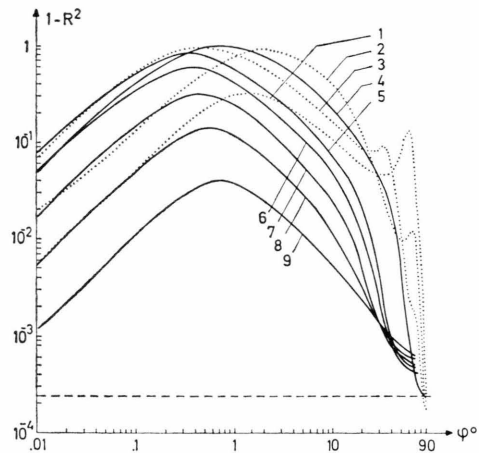

Fig. 10. Transmission coefficient vs φ for an incident TM wave for nine values of ω/ω_{ci} given in Table 2 using the parameters of Table 1.

In order to make this work pertinent to current laboratory plasmas the computations of Ref. [9] will be extended to cover a wider range of ω/ω_{ci}. Figure 10 shows the transmission coefficient for an incident TM wave for several different values of ω/ω_{ci} or ω_{pe}/ω_{ce} given in Table 2. As might be expected from the propagation condition, there is poor transmission for large values of ω_{pe}/ω_{ce}. Frequencies above the twentieth cyclotron harmonic may be considered lacking accessibility. Although there is evidence of poor coupling for the low-har-
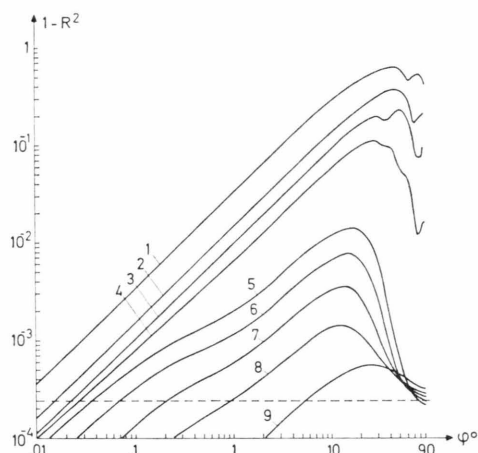

Fig. 11. Transmission coefficient vs φ for an incident TE wave for nine values of ω/ω_{ci} given in Table 2 using the parameters of Table 1.

monics (e. g., $\omega/\omega_{ci} = 2$) as well, it will be seen in Sec. IVc that transmission improves upon making the density profile less steep. In all the cases, the best coupling takes place near $\varphi \sim 1°$ which would seem to confirm the deployment of antenna configurations already arrived at in Reference [11]. Although

Table 2. Values of ω/ω_{ci} and ω_{pe}/ω_{ce} used in Figs. 10 and 11.

Curve number	ω/ω_{ci}	ω_{pe}/ω_{ce}
1	2	0.03
2	4	0.06
3	6	0.10
4	8	0.14
5	10	0.17
6	20	0.35
7	22	0.39
8	24	0.43
9	30	0.57

no clear picture is available [20] regarding the loss of transmission for very small angles, we have confirmed analytically, using a slab model of uniform low density, that no transmission indeed occurs for $\varphi \to 0$.

The curves for TE polarization displaying a more regular behaviour as a function of ω_{pe}/ω_{ce} are shown in Fig. 11 and should also be read in conjunction with Table 2.

Fig. 12. Transmission coefficient vs φ for $\omega/\omega_{ci} = 2$ ($\omega_{pe}/\omega_{ce} = 0.33$) for an incident TM wave for three different values of the profile width "g". All other parameters are those of Table 1.

(c) The Density Profile

As the profile width "g" is increased with a resultant less steep density profile, the adiabaticity condition of the WKB theory is better realized and one
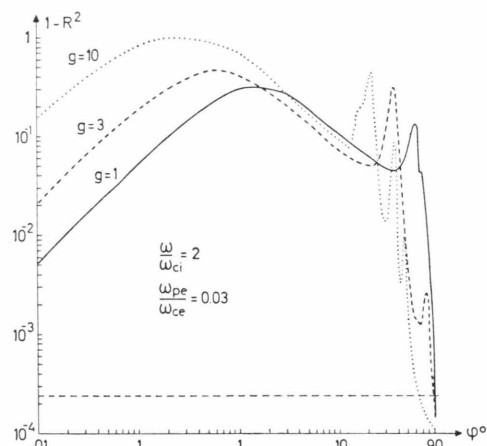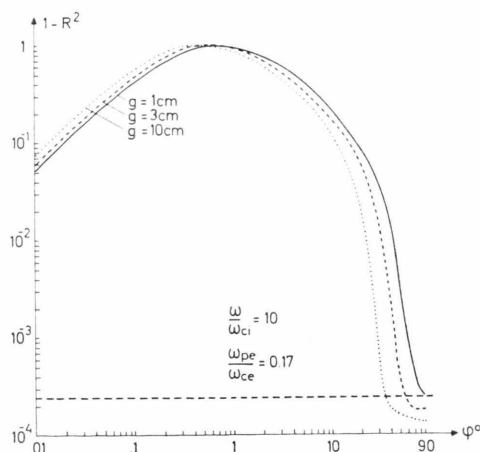

Fig. 13. Transmission coefficient vs φ for $\omega/\omega_{ci} = 10$ ($\omega_{pe}/\omega_{ce} = 0.17$) for an incident TM wave for three different values of the profile width "g". All other parameters are those of Table 1.

can expect an improvement in transmission. On the other hand an increase in the profile width enlarges any evanescent region present between the plasma edge and the hybrid layer. Evanescence increases both for increasing φ and ω_{pe}/ω_{ce}.
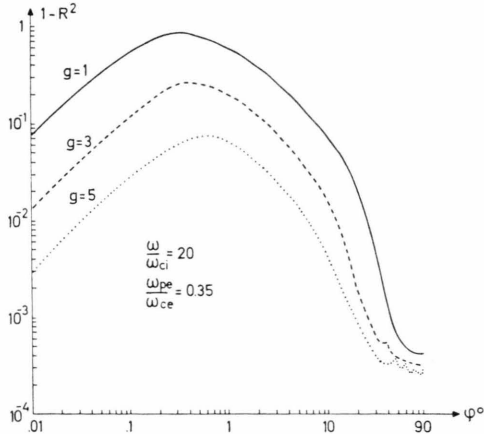

Fig. 14. Transmission coefficient vs φ for $\omega/\omega_{ci}=20$ (ω_{pe}/ω_{ce} =0.34) for an incident TM wave for three different values of the profile width "g". All other parameters are those of Table 1.

In view of the two competing effects better transmission should be obtained for small φ and ω_{pe}/ω_{ce}, while decreased transmission is to be expected for large φ and ω_{pe}/ω_{ce} as the profile width "g" is increased keeping all other parameters unchanged. These conclusions are eminently borne out in Figs. 12 – 14 drawn for three different values of ω_{pe}/ω_{ce} for an incident TM wave as well as in Fig. 15 for
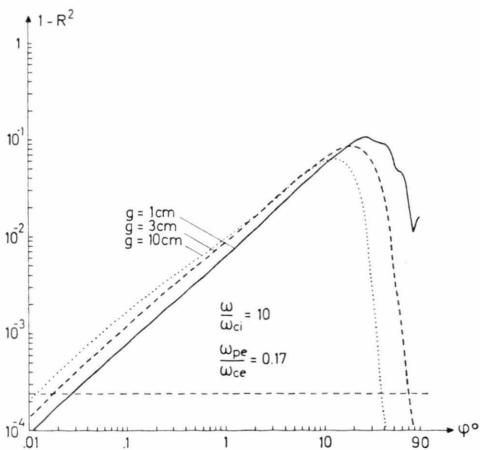

Fig. 15. Transmission coefficient vs φ for $\omega/\omega_{ci}=10$ (ω_{pe}/ω_{ce} =0.17) for an incident TE wave for three different values of the profile width "g". All other parameters are those of Table 1.

the case of an incident TE wave using ω_{pe}/ω_{ce} = 0.17.

(d) The Propagation Characteristics

The propagation constant k_x is plotted as a function of position for several φ and for three different values of ω_{pe}/ω_{ce} in Figs. 16 – 18 for both the slow and the fast waves. The unprimed and the primed curves correspond to the case $T = \infty$ ($\nu_{ei} = 0$) and $T = 3 \times 10^4$ °K, respectively. Typically there is a region of complex waves near the plasma edge which widens for increasing φ (or decreasing n_z) as well as for increasing ω_{pe}/ω_{ce}. This behaviour is easily
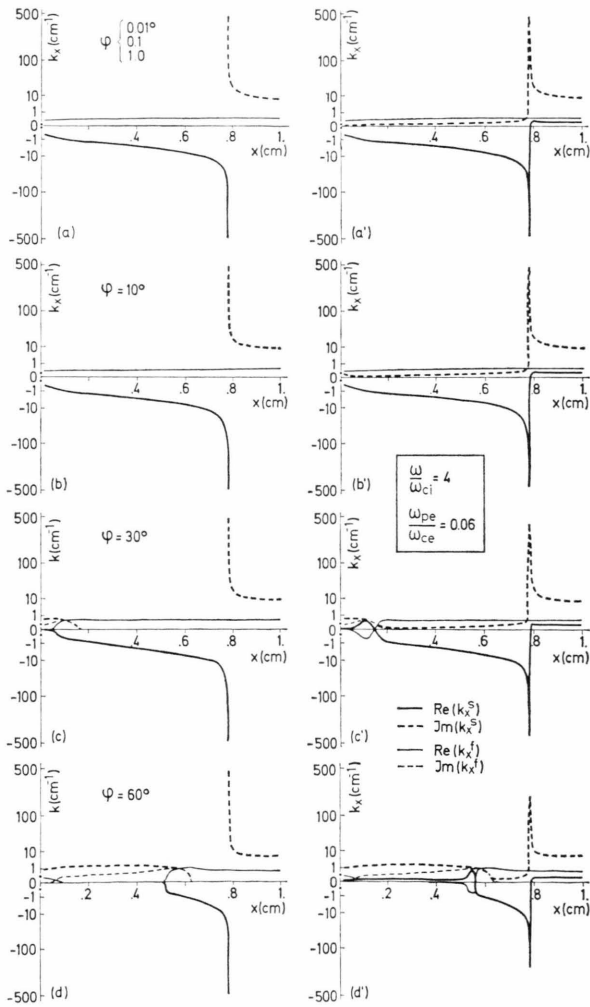

Fig. 16. The propagation constant k_x vs x for $\omega/\omega_{ci}=4$ for both the slow and the fast waves for four values of φ. The unprimed and the primed pairs are for $T=\infty$ ($\nu_{ei}=0$) and $T=3\times10^4$ °K, respectively.

understood from the following approximate expression for (2.6) near the plasma edge,

$$2 n_x{}^2 \approx (\beta\gamma - \gamma\sin^2\varphi) \pm [\,(\beta\gamma - \gamma\sin^2\varphi)^2$$
$$- 4\gamma(a^2\beta^2 + 2\beta\sin^2\varphi)\,]^{1/2} \qquad (4.1)$$

where $a = \omega/\omega_{ci} > 1$, $\beta = \omega_{pi}{}^2/\omega^2 \lesssim 1$, $\gamma = \omega_{pe}{}^2/\omega^2$, and terms of order $\sin^4\varphi$, $1/a^2$, β^2 and $1/K_\parallel$ have been disregarded. Due to the neglect of $1/K_\parallel$, (4.1) is not valid in an extremely narrow region of width $\varDelta$ (of the order $(m/M)h$ where h is the depth of the hybrid layer) near the plasma edge. $\varDelta$ is typically less than one-tenth of a millimeter for the parameters of this paper and can not play a role of any significance. This narrow region is omitted in Figs. 16 − 18 and the vacuum values of $k_x^{f,s}$ are shown as two dots on the vertical axis. These curves clearly exhibit

non-adiabatic behaviour both near the plasma edge and the hybrid resonance.

For small φ, $\sin\varphi \to 0$ and (4.1) becomes

$$2 n_x{}^2 \approx \beta\gamma \pm \beta[\gamma^2 - 4 a^2\gamma]^{1/2}. \qquad (4.2)$$

Near the plasma edge, γ^2 is small so that

$$2 n_x{}^2 \approx \beta\gamma \pm 2 i\, a\,\beta\,\gamma^{1/2} \qquad (4.3)$$

and n_x has a pair of complex conjugate solutions. For larger densities γ^2 becomes large and the solutions become real when

$$\gamma^2 \gtrsim 4\, a^2\,\gamma$$
$$\text{or} \quad \omega_{pe} \gtrsim 2\,(\omega/\omega_{ci})\,\omega\,. \qquad (4.4)$$

Thus, if ω_{ci} is kept fixed, the region of complex waves increases for larger values of ω/ω_{ci} as can also be seen from Figs. 16 a − 18 a. For larger values of φ, the factor $-\gamma\sin^2\varphi$ contributes an additional negative part to $2 n_x{}^2$ resulting in yet larger regions of complex waves.

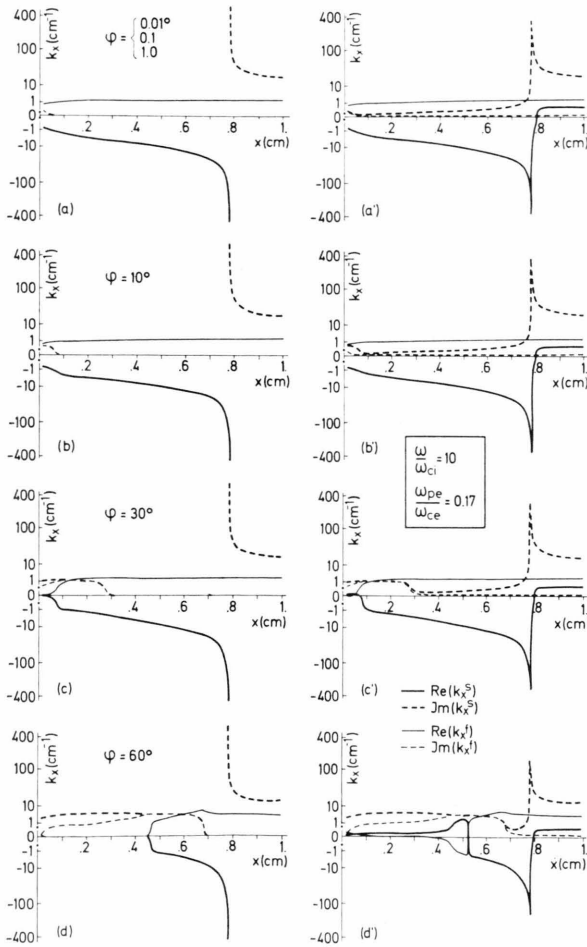Fig. 17. The propagation constant k_x vs x for $\omega/\omega_{ci} = 10$ for both the slow and the fast waves for four values of φ. The unprimed and the primed pairs are for $T = \infty$ $(\nu_{ei} = 0)$ and $T = 3 \times 10^4$ °K, respectively.
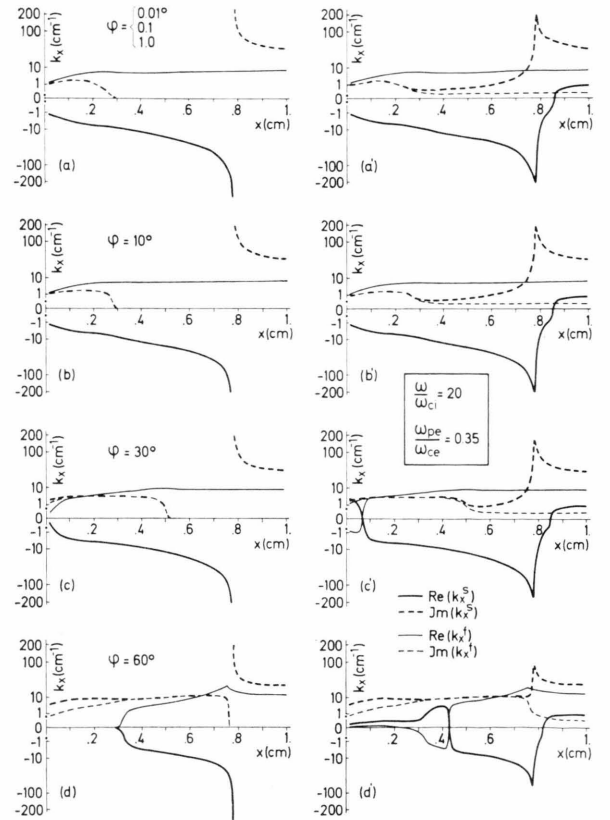

Fig. 18. The propagation constant k_x vs x for $\omega/\omega_{ci} = 20$ for both the slow and the fast waves for four values of φ. The unprimed and the primed pairs are for $T = \infty$ $(\nu_{ei} = 0)$ and $T = 3 \times 10^4$ °K, respectively.

A similar expansion of (2.6) for higher densities would expose that while one of the roots of n_x^2 displays a resonance as $K_\perp \to 0$, the other root is relatively unaffected by the presence of the hybrid layer [1-3].

The most important conclusion of this section is that for the case $n_z < 1$, the region of evanescence near the plasma edge is narrowest for small angles of incidence, in which case the width of the evanescent region deducable from (4.4) is seen to be the least for small values of ω/ω_{ci}.

5. Discussion

The principal motivation for this work was to determine whether it is possible to gain accessibility to the lower-hybrid resonance in a plasma of thermonuclear parameters under the restriction $n_z < 1$, in which case it would be possible to couple rf energy into propagating waveguide modes [9] using simple waveguide coupling techniques. This approach to coupling has the important advantage that no structures or coils are required to be built inside the reactor walls thereby obviating the attendent technical difficulties [21].

The most significant result obtained is that for $\omega_{pe}/\omega_{ce} \lesssim 0.4$ and $\varphi \sim 1°$, the TM vacuum wave is almost completely transmitted into the plasma. Since both the electric and the magnetic fields of the wave, for the above case, are transverse to the z-axis (the static magnetic field direction), the field configuration is reminiscent of TEM waves in a co-axial waveguide. Thus in a small laboratory plasma, a current loop oriented to produce an azimuthal rf magnetic field will launch waves which will easily couple into the plasma. In a larger machine where the free-space wavelength of the rf field exceeds the transverse machine dimensions, the optimum antenna will consist of a waveguide with its axis along the magnetic field direction and the short dimension perpendicular to the plasma surface. As discussed in Ref. [11], in a large machine, the antenna problem may indeed be uncritical: the part of the energy not at once transmitted into the plasma will bounce back and forth between the plasma and the metal wall, because due to the large machine dimensions involved, propagating modes could exist in the vacuum region between the plasma and the metal wall. Given a better possibility of penetration into the plasma compared to the metal wall, this coupling would be affected with a high efficiency.

For easy reference ω_{pe}/ω_{ce} and the lower-hybrid frequency f are plotted as a function of plasma density and magnetic field in Figure 19. It is then
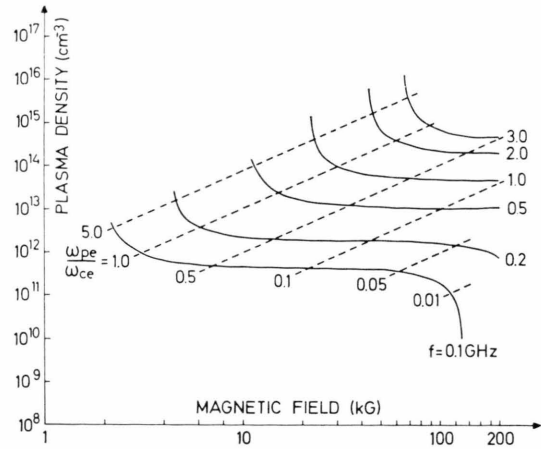

Fig. 19. The curves showing ω_{pe}/ω_{ce} as well as the lower-hybrid frequency f as functions of plasma density and magnetic field for deuterium. Region of accessibility corresponds to $\omega_{pe}/\omega_{ce} \lesssim 0.4$.

possible to learn at a glance the minimum static magnetic field B_0 necessary for accessibility (i. e., $\omega_{pe}/\omega_{ce} \lesssim 0.4$) for any given plasma density. Perhaps, an easier way to define the region of accessibility is by noting that wave penetration occurs for $\omega/\omega_{ci} \lesssim 20$. We do not hazard a guess as to the pertinence of the accessibility criteria developed in this paper for a hot plasma. However, it has been claimed by several authors [23-26] that propagation from the plasma edge till the hybrid layer is not materially affected by the inclusion of finite temperature effects. In that case, an obvious inference from the present results is that all the ion-cyclotron harmonics from the second till the twentieth are accessible to TM vacuum waves incident at small angles on the plasma surface. In a torus machine, it is not feasible to heat the plasma above the tenth ion-cyclotron harmonic even for tori of large aspect ratio if one wishes to avoid heating near the plasma edge. One may then, in fact, say that lower-hybrid resonance and consequently the ion-cyclotron harmonics are accessible for thermonuclear parameters as was already concluded in the preliminary results of Reference [11].

The above observations, namely that penetration occurs for small φ and ω_{pe}/ω_{ce} supports the contention that there should not be a substantial region of evanescence between the plasma edge and the hybrid

layer, i. e., $|\mathrm{Im}(\int_0^h n_x \, dx)|$ should not be too large. The converse, however, is not true. The wave may be almost completely reflected (see Figs. 10 and 11 for $\varphi \to 0$) even though k_x is real (Figs. 16 – 18) practically over the entire region $0 < x < h$. Therefore only the comprehensive concept incorporating the propagation condition *and* taking into account the lack of adiabaticity would constitute a valid definition of accessibility.

In conclusion we believe that this paper should bring us to a better understanding of the problem of lower-hybrid penetration and provide the experimentalist an elegant and technically simple solution for coupling rf energy to a plasma. The ultimate fate of the coupled energy in a hot plasma, the complex nonlinear and parametric effects due to the buildup of inevitably large localized electric fields, as well as the effect of complicated particle trajecteries across magnetic field gradients in a torus, are but a few of the questions which must be settled before a fully satisfactory understanding of rf heating of thermonuclear plasmas can emerge.

Acknowledgement

[1] T. H. Stix, Theory of Plasma Waves, McGraw Hill, New York 1962.

[2] R. Parker, QPR No. 102, Res. Lab. of Electronics, MIT, Cambridge, Mass. **97**, [1971].

[3] V. E. Golant, Zh. Tekh. Fiz. **41**, 2492 [1971]; Sov. Phys. Tech. Phys. **16**, 1980 [1972].

[4] Since in an actual reactor, the transverse dimensions of the apparatus would exceed the free-space wavelength of the rf source, Derfler has suggested (in the somewhat different context of enhancing Landau damping of Bernstein modes) coupling to the slow waves by constructing a slow-wave structure within the reactor walls (communicated to the "Advisory Group on Plasma Heating", Grenoble, March 29—31, 1971).

[5] K. G. Budden, Proc. Roy. Soc. (London) **A 227**, 516 [1955].

[6] From Ref. 2, p. 105, the differential equation for the electric field is

$$\frac{\partial^2 E_z}{\partial x^2} - \frac{K_\perp'}{K_\perp} \frac{n_z^2}{K_\perp - n_z^2} \frac{\partial E_z}{\partial x} + k_0^2 \frac{K_\parallel}{K_\perp} \, (K_\perp - n_z^2) E_z = 0 \, .$$

Near the plasma edge it is readily shown that the ratio ξ of the second to the last term is given by

$$\xi \sim 0 \left| \frac{\lambda_0}{2 \pi h} \frac{n_z^2}{(1 - n_z^2)^{3/2}} \right| \, ,$$

where λ_0 is the free-space wavelength of the rf field and h is the depth of the hybrid layer measured from the plasma edge. From this equation it is clear that the assumption $\xi \ll 1$ is not permissible in any case of practical interest.

[7] V. Agnello, D. Colombant, P. Fieffe-Prevost, G. Ichtchenko, and S. Kulinski, IV-ECCFPD, Rome 1971, p. 131.

[8] S. S. Pešić, Nuclear Fusion **11**, 461 [1971].

[9] S. Puri and M. Tutter, Nuclear Fusion **13**, 55 [1973].

[10] The case $n_z > 1$ will be studied in a forthcoming publication.

[11] S. Puri and M. Tutter, Z. Naturforsch. **28 a**, 438 [1973].

[12] L. Spitzer, Jr., Physics of Fully Ionized Gases, Interscience Publishers, New York 1962.

[13] This should not be taken as a confirmation of the WKB theory because the transmission coefficient drops rather rapidly (Fig. 10) for smaller angles ($\varphi = 0.1°$, $0.01°$) although the propagation constant k_x remains practically unchanged (see Figure 17 a′).

[14] This is true only if $\langle \nu_{ei}\rangle/\omega \lesssim 10^{-2}$ as is the case here. For appreciably higher values of $\langle \nu_{ei}\rangle/\omega$, strong collisional absorption takes place well ahead of the hybrid layer nearer to the plasma edge.

[15] H. H. Kuehl, Phys. Fluids **5**, 1095 [1962]; R. K. Fischer and R. W. Gould, Phys. Rev. Letters **22**, 1093 [1969].

[16] The horizontal axis "z" in Fig. 7 of Ref. 9 is scaled incorrectly.

[17] In subsequent sections IVb and IVc it will be seen that the transmission coefficient decreases for very small incidence angles as well.

[18] S. Puri, F. Leuterer, and M. Tutter, J. Plasma Phys. **9**, 89 [1973].

[19] For a given gas, ω/ω_{ci} and ω_{pe}/ω_{ce} are uniquely related (see Table 2 for deuterium).

[20] Although the results of Parker [2] and Golant [3] would seem to confirm the $\varphi^{2/3}$ dependence of $(1-R^2)$ in Fig. 10, the agreement is fortuitous in the light of the comments made in the introduction and Footnote 6.

[21] Briggs and Parker [2, 22] have also suggested an antenna requiring no structures within the machine and consisting of a rectangular waveguide flush mounted on the torus wall with its short dimension parallel to the magnetic field direction. However, due to an oversight in their analysis (see Sec. I), it is not clear whether this scheme would be valid if the short circuiting effect of large longitudinal electron conductivity on the imposed tangential field E_z of the waveguide is correctly taken into account.

[22] R. J. Briggs and R. Parker, Phys. Rev. Lett. **29**, 852 [1972].

[23] T. H. Stix, Phys. Rev. Letters **15**, 878 [1965].

[24] A. D. Piliya, Zh. Tekh. Fiz. **36**, 818 [1966]; Sov. Phys. Tech. Phys. **11**, 609 [1966].

[25] A. D. Piliya and V. I. Fedorev, Zh. Eksp. Teor. Fiz. **57**, 1198 [1969].

[26] V. M. Glagolev, Plasma Phys. **14**, 301 [1972].